Worcester Polytechnic Institute
Digital WPI

March 2013

Design and Construction of a Velocity Probe Calibration Rig

Daniel J. Frodell
Worcester Polytechnic Institute

Ethan E. Deragon
Worcester Polytechnic Institute

Paul David Ciolek
Worcester Polytechnic Institute

Stephen Joseph Kressaty
Worcester Polytechnic Institute

Follow this and additional works at: https://digitalcommons.wpi.edu/mqp-all

Design and Construction of a Velocity Probe Calibration Rig

A Major Qualifying Project Report

Submitted to the Faculty of
WORCESTER POLYTECHNIC INSTITUTE
In partial fulfillment of the requirements for the
Degree of Bachelor of Science

By

Paul Ciolek
Ethan Deragon
Daniel Frodell
Stephen Kressaty

3/1/2013

Advisor: Professor Simon Evans

Acknowledgements

Our Team would like to express our most sincere appreciation to the following individuals and companies. Without their knowledge, enthusiasm, and dedication, our project would not have been possible.

Prof. Simon Evans – For his advice, guidance, and patience with our project team throughout the entirety of the project.

Kevin Arruda – For his assistance with machining of aluminum plates, 80/20 stock, and aluminum rod components.

Greg Overton - For his assistance with machining of out tooling board and motor sprocket components.

Barbara Furhman – For assisting the team with obtaining all necessary parts, and equipment to complete our project.

Prof. Ken Stafford – For his advice in regards to motor selection, and also building a motor controller.

Prof. Mark Richman – For his help with the stress and deflection analysis of the probe manipulator component.

Prof. Stephen Nestinger – For providing advice on how to design a mechanism that allows for rotation along two axes.

Norm Into – For his recommendations for an axial fan blade profile and advice with the multi-wing fan blade selection software.

Gray Metal Products – For the manufacturing of the flow channel section of the project.

Associated Builders Inc. – For assistance with the augmenting of the prefabricated flow channel section, and supply of materials and fasteners.

Abstract

This report describes the design and construction of a velocity probe calibration rig to be used in future fluids research at Worcester Polytechnic Institute. A high accuracy, automated device was manufactured with the capability of taking flow measurements over a wide range of testing conditions. This instrument was designed to collect low speed airflow measurements from a probe over a range of pitch and yaw angles, with both pressure probes and hot wire anemometers. The major components of this device included a flow channel, probe manipulator, and an axial fan drive system. The probe manipulator was designed to provide greater than $\frac{1}{10}$ degree positioning accuracy, and repeatability in fluids experimentation.

Table of Contents

Table of Figures

List of Tables

1 Introduction

Probe calibration allows for high accuracy measurement of flow parameters, and is particularly important in experimental fluids applications. Effective probe calibration equipment needs to be suitable for a variety of probe types and have a high resolution in probe positioning, in order to produce high accuracy experimental measurements. Automation of probe calibration devices ensures that the testing equipment will have the same variation under the same testing conditions and also eliminates the need for manual positioning of probes.

The probes used in fluids velocity measurement require calibration over a range of angles, so that velocity components can be measured in complex flow fields. The ideal design for a probe calibration rig would have an unlimited range of pitch and yaw combinations for the probe holder manipulator, as well as an infinitesimal degree of accuracy. For wind tunnel testing purposes, ±90 degrees of pitch and yaw are sufficient for flow analysis. The reliable operating range for these probes, however, is limited to angles of pitch and yaw not exceeding 30 degrees (Díaz et al., 2008). While a probe manipulator may be capable of achieving a larger range in positions, measurement data taken beyond the 30 degree operating range will have higher errors.

Probe positioning in the Gas Turbine Research Lab (GTRL) at Worcester Polytechnic Institute is currently restricted to pitch, over a range of approximately ±20 degrees (Baiense et al., 2012). The positioning process consists of adjusting the probe holders by hand to an flow angle measured with an inclinometer. This process is prone to human error, making it both inconsistent and imprecise. The proposed solution to this problem is to automate the positioning process through the use of high precision rotary tables with an open loop feedback system formatted in LabView.

The design and construction of an automated probe manipulator with multiple degrees of freedom explored by researchers T.F. Hu and Y.Y. Hsu, resulted in the development of a device with 7 degrees of freedom including both pitch and yaw. Rotary tables provided a foundation to the device that allowed for positioning accuracy on the order of a tenth of a millimeter (Hu & Hsu, 1994).

In an effort to improve testing in fluids research at WPI, an automated rig was designed and commissioned for use in the GTRL at WPI. Operational and maintenance procedures specific to the rig are detailed later in the report and recommendations are included to improve the performance of the rig as a whole. The final design and construction of the velocity probe calibration rig are discussed with the aim of illustrating how this project was successful in furthering the experimental capabilities of the GTRL at WPI.

2 Objectives

The objectives of this project are below:

2.1 Project Goals

- Further the experimental capabilities of the Gas Turbines Research Laboratory at WPI by
  constructing a velocity probe calibration rig for fluids researchers.

2.2 Requirements

- Must be able to test probes placed parallel to the flow and perpendicular to it.

- Air flow velocity through the flow channel must reach a minimum of 32 m/s.

- Must be able to accurately manipulate probes to desired angles to within $\frac{1}{10}$ of a degree,
  in a repeatable fashion.

2.3 Constraints

- Must be able to be move between the Gas Turbines Research Laboratory and the Fluids
  Laboratory in Higgins Labs at WPI.

- Flow Channel section should have removable sections that house flow conditioning
  screens and honeycombs.

2.4 Criteria

- Device should be able to move fluid to a velocity of 55 m/s at the probe to fully simulate
  the abilities of the recirculating wind tunnel in the Fluids Laboratory.

- Device should be able to reach a full 180 degrees of both pitch and yaw.

- Device should be able to calibrate both a 5-hole pressure probe and 3-wire hotwire
  anemometer over their effective ranges.

- The flow incident on the velocity probe should have a turbulence of less than 0.5%.

3 Background

In this section, blower-type wind tunnels are described. Of the many types of wind tunnels used in aerodynamics research, this is the design most relevant to the design of a calibration rig.

3.1 Blower-type Wind Tunnels

This section details the significance of each of the components of blower-type wind tunnels, and also provides motivation for decisions made in the design section of the paper. Figure 1 shows a dimensioned sketch of a blower type wind tunnel, powered by a centrifugal blower. Centrifugal blowers are generally used to move smaller volumes of fluid at higher static pressures, whereas axial flow fans are used to pass larger volume flowrates at lower static pressures (Dixon & Hall, 2010).
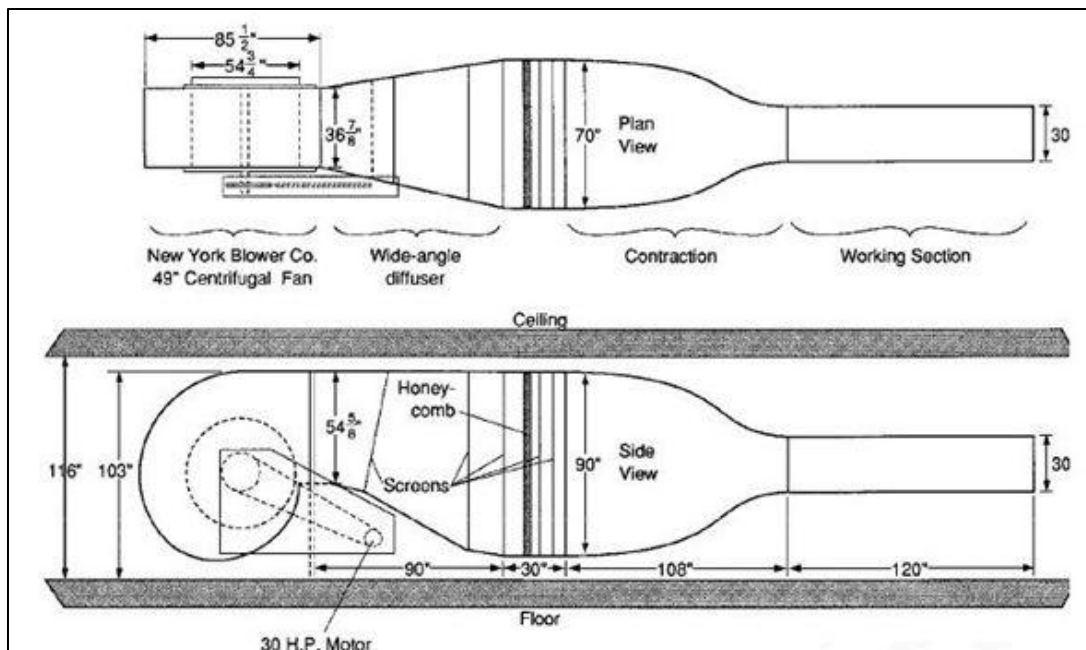
Figure 1: Blower Type Wind Tunnel (Roshdy, 2013)

The components of open return blower-type wind tunnels are detailed in the following subsections beginning with the test section and ending with the inlet of the tunnel.

3.1.1 Test Section

Wind tunnel test sections serve as the control volumes for fluids research experiments and are used to house instrumentation for collecting flow measurements. In the blower-type tunnel, the test section may either be located at the exit of the tunnel. Several precautions need to be taken when designing blower type wind tunnels in order to produce the desired airflow in the tunnel test section. Care must be taken in the design to limit the turbulence in the test section. Unintended turbulence is the largest source of error within these types of wind tunnels (Pankhurst & Holder, 1952). Sources of turbulence include, but are not limited to: fans, boundary layers, and contractions in the wind tunnel walls.

To limit the influence of the boundary layer turbulence on the testing section, the area of this section must be large enough such that the flow measurements are taken outside of the boundary layer thickness. Turbulence and nonlinearities attributed to the fan are corrected with the addition of honeycombs and screens in the flow channel of the tunnel. Reducing the turbulence from contractions can be done by modeling the contraction curve by a higher order polynomial or by following the design by eye method (Pope & Rae, 1984).

3.1.2 Contractions

Contractions serve a two-fold purpose in wind tunnels by both increasing the mean velocity of the flow, and also reducing the mean velocity fluctuations (Martin, 2006). Contractions located downstream of the flow channel also provide a reduction in the size of turbulent eddies that are created as the flow passes through the screens. Longer contractions allow for a gradual transition from the one area to another, and are better able to limit the pressure drop of the screens in the flow channel, making them preferable to shorter ones.

A case study performed by Doolan (2007) at the University of Adelaide reviewed two contraction designs based on higher order polynomial approximations of the curve of the contraction. The study found that a 5th order polynomial contraction design produced the best results yielding greater than 99.5% flow uniformity in the test section (Doolan, 2007). The optimal shape and dimensions can be determined using computational methods such as those described above, but more often than not designers will machine a contraction for a required area ratio, otherwise known as the design by eye method (Pope & Rae, 1984).

3.1.3 Honeycombs and Screens

Screens create flow uniformity in wind tunnels by reducing boundary layer growth and reducing differences in the flow velocity gradient (Pope & Rae, 1984). These components work by inducing a pressure drop, proportional to the square of the axial velocity. Higher velocities are therefore reduced more than lower velocities, thus creating a more uniform velocity distribution (Mehta & Bradshaw, 1979). The downside to using screens to improve flow quality is that they result in pressure losses. The pressure losses associated with screens require an increase in the power provided by the motor of the axial fan (Pope & Rae, 1984). This pressure loss is also important for determining the location of the screens within the tunnel. Screens should be placed in a location in which the velocity of the flow is the lowest, so as to introduce the least amount of pressure loss and therefore reduce the power requirement of the fan. It is for this reason that wind tunnels usually have a large cross-sectional area flow channel or settling chamber, in which the cross sectional area is increased to reduce the velocity through the screens.

Honeycombs function to reduce the lateral turbulence in the flow by forcing small sections of the flow to straighten through small, tube-like cells. Mehta and Bradshaw (1979) have suggested that

honeycombs are most effective when the length of the honeycomb is 6-8 times the size of an individual cell. In light of the fact that honeycombs produce slight axial turbulence in the flow, Mehta and Bradshaw have recommended positioning honeycombs upstream of screens. This formation allows for the reduction of both axial and lateral turbulence (Mehta & Bradshaw, 1979).

3.1.4 Settling Chambers

Settling chambers are the sections of the wind tunnel that house the honeycomb and screen components, and are essential for correcting non linearities in the flow. Screens and honeycombs calm the large turbulent eddies present upstream, but they also produce smaller turbulent eddies downstream as well. The length of the settling chamber also acts as a secondary means of reducing these leftover flow disturbances. This holds true, since flow turbulence is inversely proportional to the distance the flow travels in the stream-wise direction (Mehta & Bradshaw, 1979).

Mehta and Bradshaw specified in their *Design Rules for Low Speed Wind Tunnels* that the minimum distance between any two screens in a flow channel must be at least one-fifth the size of the major dimension of the settling chamber, in order to for them to retain the effectiveness of the screens.

3.1.5 Inlet Diffuser

The function of the inlet diffuser component is to expand the flow field generated by the fan or blower into the settling chamber, while recovering static pressure (Pope & Rae, 1984). In other words, the diffuser expands the flow by decreasing flow velocity and increasing cross-sectional area of the channel, according to the laws of continuity.
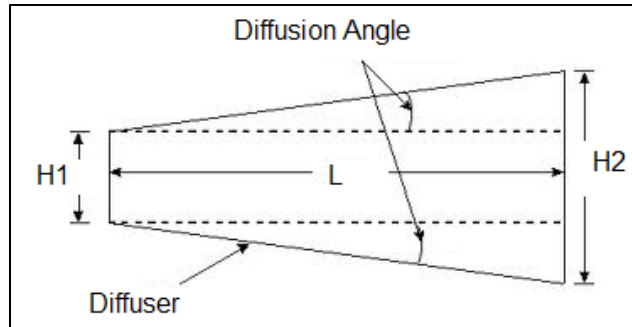
Figure 2: Inlet Diffuser Sketch

The geometry of the diffuser section must be carefully constrained, to avoid flow separation at the corners of the section, as well as the diffuser exit. Two requirements must therefore be satisfied in order to avoid separation within the diffuser section. Firstly, the diffuser angle should not exceed seven degrees of inclination with respect to the horizontal. At angles that are more extreme than this, flow separation occurs, and the flow loses its uniformity. Secondly, the ratio of the exit area to the inlet area should be kept on the order of approximately 2.5 to 1, or at most 3 to 1 (Pope & Rae, 1984), or separation again occurs.

3.2 Flow Measurement

The following sections explain the purpose and use of hot wire probes and pressure probes, including their calibration. The impact of probe calibration on rig design will also be discussed.

3.2.1 Hot wire Anemometers

Hot wire anemometry (HWA) probes can include anywhere from one to three wires, with the number of wires specifically corresponding to the number of components of the flow velocity that are to be measured. While a single wire probe can only be used to obtain the velocity component normal to the wire, three-wire probes can determine the full vector definition of velocity at a point in the flow field. An image of a three wire probe can be seen in Figure 3 below.
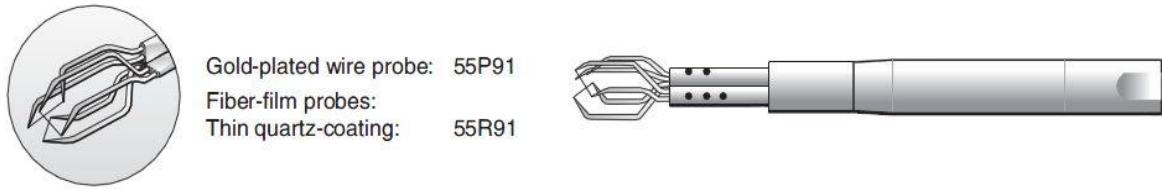
Figure 3: 3-Wire Hot Wire Probe (Dantec Dynamics)

Hot Wire Anemometry (HWA) is used to measure velocity. An electric current is run through a thin wire, and the wire is then heated by the current. The wire is then cooled by a flow passing over it, resulting in a change of resistance which is used to identify the flow velocity (Comte-Bellot, 1976). The most popular form of HWA, constant temperature mode, involves keeping the hot wire probe at constant temperature, then exposing it to a flow velocity, which is then recorded as a voltage difference measured across the wire. Keeping the probe at a constant temperature allows for accurate measurements over a wide range of velocities, which greatly increases the range the probe can measure (Bruun, 1995).

There are certain problems that may occur with HWA. One problem with hot wire anemometers is that they are prone to dust disruption. Over time, dust accumulates on the HWA, causing the calibration characteristics to change, requiring the probe to be recalibrated (Bruun, 1995). Heat generated by the current passing through the wire can also skew the calibration characteristics. These problems are easily resolved by regular calibration of the HWA (Bruun, 1995).

3.2.2 Pressure Probes

Multi-hole pressure probes are commonly used to gather flow velocity data through a number of separated channels. For a three-hole probe, pressure differences will occur between the upper and lower channel for any incident flow direction that is non-zero [see Figure 4]. These pressure differences are then used to determine velocity and flow angle in one plane of the flow. A five-

hole probe, on the other hand, has two additional channels mounted on the left and right of the center port, making it capable of measuring pitch, yaw, and velocity. Similar to a 3-wire hotwire anemometer, a five-hole pressure probe allows for the determination of the full vector definition of the velocity. The function of the center hole in multi hole pressure probes is to measure stagnation pressure over precise operating ranges. Outside of these ranges, the central hole can still be used to determine the flow velocity vector if properly calibrated.
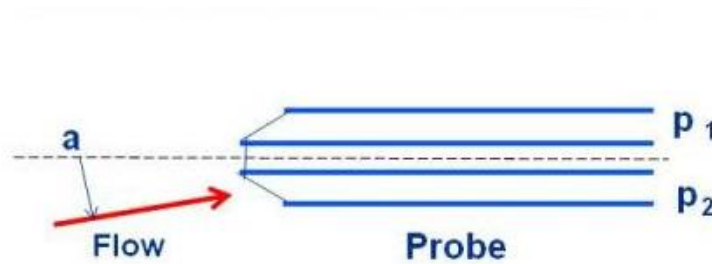
Figure 4: Flow creating pressure differences across a probe head

Calibration of a pressure probe, which is necessary for accurate results, consists of mounting the probe head to a test section providing clean flow of a known axial velocity. The probe head is then oriented at various known angles of pitch and yaw while collecting pressure measurements from each pressure port. This data yields a calibration curve that relates the pressure differences to known velocities and orientations (Paul et al., 2011). The calibration of a 3-wire HWA follows a similar process.

3.2.3 Probe Calibration Studies

It is important to understand the operational limits of probe equipment, to ensure that the flow measurements taken during testing are reasonable. Díaz et al. (2008) conducted a study investigating these limits for cylindrical pressure probes. Previous studies examining multi-hole pressure probe ranges concluded that these probes were functional up to ranges of ±30 degree

17

due to discontinuities in calibration coefficients. A new calibration procedure was presented in this study, which showed that an improved range of ±70 degrees could be achieved. These results emphasize the importance of having probe manipulator mechanisms that are capable of a wide angle variation (Díaz et al., 2008).

Another study conducted by Van Dijk and Nieuwstadt (2004) reviewed calibration methods for 4-hole velocity probes, with the aim of finding a reliable method for determining the component of a turbulent velocity vector. The overarching goal of the study was to find a method that could estimate the turbulence velocity vector to within 10% accuracy (van Dijk & Nieuwstadt, 2004). Their probe manipulator mechanism relied on D.C. motors with accuracies of 0.15 and 0.1 degrees in the pitch and yaw directions respectively, and was capable of an angular variation of ±40 degrees. The authors concluded that many of the calibration methods examined provided large systematic errors, and recommended that the prior studies reevaluate their calibration methods and operation of equipment. The results of this study illustrate the importance of reliability in measurements as well as the importance of having high accuracy equipment.

3.2.4 Probe Manipulation

In 1993, Hu and Hsu undertook a study to design and construct a probe manipulator with seven degrees of freedom. The purpose of this study was to provide researchers with a blueprint for a high accuracy, closed loop controlled mechanism that allows for measurement repeatability. These degrees of freedom, including roll, pitch, yaw, and translation of the probe manipulator in the x-, y-, and z-directions. The achievable angular range of this design was better than $\pm 45°$ in both pitch and yaw.

The design objectives of this study were to provide translation and rotation about three axes with positioning accuracy within 0.1 mm. The probe manipulator design employs worm-gear driven rotary tables, along with a closed feedback loop implemented by a servomotor, resulting in excellent repeatability, as well as a positioning accuracy of approximately 0.02 - 0.05mm (Hu & Hsu, 1994).
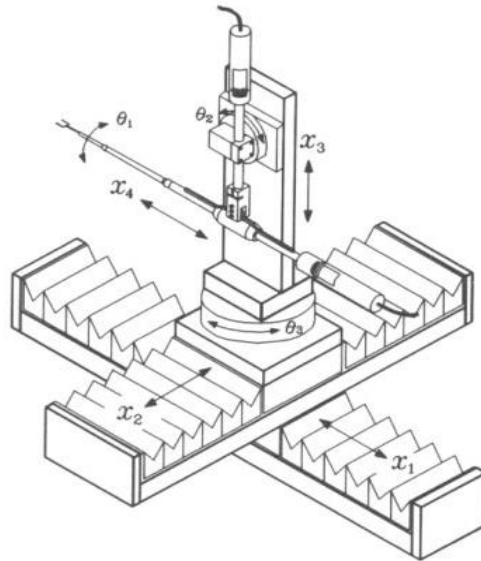
Figure 5: Probe Manipulator Design with Seven Degrees of Freedom (Hu & Hsu, 1994)

From this study conducted by Hu and Hsu (1993), and those described in section 3.2.3, it is clear that the desirable characteristics of a probe manipulator include: having a wide angular range, being able to operate with several degrees of freedom, and lastly, having measurement repeatability with high accuracy capabilities. The next section of this report will address each of these characteristics with the design of this component.

4 Design

This portion of the paper details the finalized design of the velocity probe calibration rig and also provides a basis for all design decisions that were made.

4.1 Flow Channel

This flow channel was designed according to the requirements presented in the background section 3.1, but was also modified to meet the manufacturing capabilities of the various manufacturers. The height and width of this component were the largest constraints in the design, since the rig as a whole needed to be portable between research laboratories at WPI.

4.1.1 Flow Channel Manufacturer

Gray Metal Products, a heating and air conditioning manufacturer from Avon, NY, was chosen for the manufacturing of the flow channel component for a variety of reasons. The first and foremost was because they offered to construct the flow channel for no cost. This company was an ideal choice also because they are experienced in manufacturing sheet metal products for air ventilation applications.

The interior surface of the flow channel was a design concern, since boundary layer growth is a problem in the test section. To ensure that the surface of the flow channel on the inside was smooth, the interior was surface treated through sandblasting, and any surface imperfections were coated with a ducting sealant.

4.1.2 Interior Dimensions

Our objective was to have a flow channel capable of producing a flow velocity ranging from 1-55 m/s, in order to cover the flow velocity range of all the wind tunnels at WPI. The final test

section diameter of 4″ was decided upon after taking into account boundary layer growth, and the manufacturing capabilities of the manufacturer. The relationship between the inlet size of the flow channel and flow velocity at the inlet was given from the mass conservation equation. That relationship and is represented graphically in Figure 6 below, which shows inlet velocity variation as a function of inlet diameter, for a test section velocity of 55 m/s. This figure was helped provide a picture of how large the flow channel was going to be as a whole. The inlet diameter chosen for the design was 12.5″, which corresponded to an inlet velocity of 4.3 mps. After consulting the product catalog of the flow channel manufacturer, the inlet diameter choice was refined to 12″, which corresponded to an inlet velocity of 4.65 m/s.
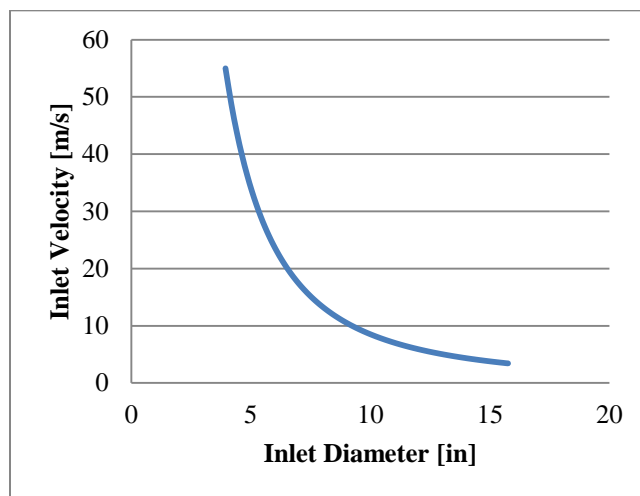
Figure 6: Inlet Flowrate Curve for $V_{Test\ Section} = 55$ m/s

The streamwise lengths of the settling chamber, the inlet diffuser, contraction and test section were limited as much as possible in the interest of spacial and cost considerations. The final length of the entire flow channel was approximately 4′, 4″ long, with a wall thickness of $\frac{1}{16}$″. Figure 7 shows the flow channel design model that was sent to the manufacturer complete with a fully dimensioned drawing in Solidworks 2011.
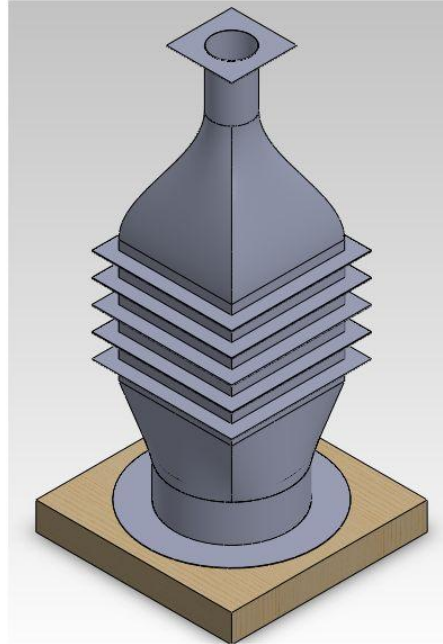
Figure 7: 12″ Flow Channel Design

The test section dimensions were determined by performing a boundary layer analysis on the

walls of the flow channel. The walls of the test section were approximated as flat plates. The

boundary layer thickness was determined to be 0.163″, under the worst case assumption that the

flow was turbulent (White, 2011). This analysis yielded a boundary layer thickness for the

designed velocity through this section. After adding a safety factor length to the boundary layer

thickness, the test section diameter was determined to be 4″, which corresponded to a test section

area of 12.6 in^2.

4.1.3 Flanges vs. Filter Racks

Since screens require cleaning because of their affinity for dust particles, the flow channel

requires detachable sections that allow the screens to be removed. Two proposals were

considered for how to satisfy this requirement; one suggested using flanges to hold the screens

fixed in place, while the other suggested taking advantage of the filter rack products in the Gray

Metal Products parts catalog to hold the screens in place. The first option was decided upon in

the end, because it decreased the length of the channel section by a full 8″ and also simplified the manufacturing process. The axial lengths of these flanged sections housing the screens were 3″.

4.1.4 Bell Mouth Design

The flow channel manufacturers were not able to manufacture the bell mouth component, due to the inlet curvature; therefore a separate piece was designed out of tooling board material. Tooling board was decided upon because it was readily available in the GTRL, and also because it was straightforward to shape. Figure 8 shows the Solidworks model of the tooling board bell mouth component. The figure shows a radius on the interior of this piece, to allow airflow to enter the flow channel with a uniform distribution. The flow channel was designed to include a flange at the inlet section which could be mounted to the tooling board piece. The inner diameter of the tooling board was 12″, in order for the attachment between the two pieces to be coincident along the inner circumference.
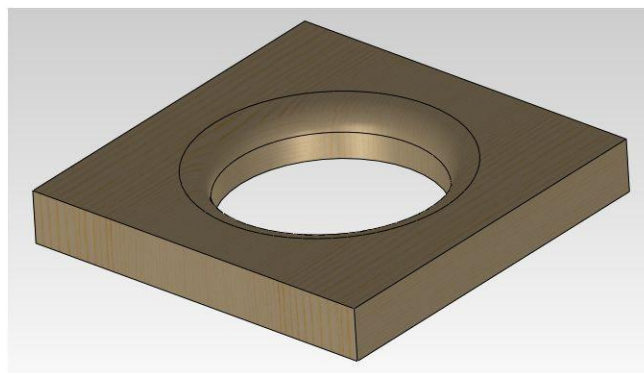
Figure 8: Tooling Board Bell Mouth Section

4.2 Screens and Honeycombs

Choosing the appropriate combination of screens and honeycombs for the flow channel first required the calculation of the loss coefficient and turbulence reduction factor desired. For the

screens and honeycombs to function properly, their placement within the flow channel must cater to certain criteria.

Mehta & Bradshaw defined the loss coefficient, K, as the change in pressure divided by the dynamic pressure. This coefficient can be approximated for each screen using the Reynolds number for the airflow, and the geometry of the screens. K is determined by the equation below.

$$K = \left(\frac{1 - 0.95 * \beta}{0.95 * \beta}\right)^2 + \frac{55.2}{R_d}$$

[1]

Where β is the open area ratio defined below,

$$\beta = \left(1 - \frac{d}{M}\right)^2$$

[2]

In these equations R_d is the Reynolds number based on wire diameter, d is the wire diameter and M is the mesh length. The K value of honeycomb is determined by the structure of the honeycomb, with hexagonal honeycomb being the most common and having a value of 0.20.

Turbulence reduction, f, is defined by Rae & Pope (1984) as the ratio of the turbulence with flow correction to the turbulence without flow correction. The turbulence reduction of a particular screen is approximated by the following equation.

$$f = \frac{1}{1 + K}$$

[3]

If multiple screens are in use, f is the product of the value of f for each screen. Honeycombs have a slightly different approximation for f, as shown below.

$$f = \frac{1 + \alpha - \alpha * K}{1 + \alpha + K}$$

[4]

Where,

$$\alpha = \frac{1.1}{\sqrt{1 + K}}$$

[5]

Using these equations to find the minimum pressure loss and the minimum settling chamber length, an appropriate combination of screens and honeycombs was found. The combination of three identical screens that have a β value of 0.46 and a wire diameter of $0.016''$ with one hexagonal honeycomb was found to be most effective for this application. This means that a $12''$ square settling chamber must be a total of about $10''$ long.

Mehta and Bradshaw (1979) noted that placement of flow conditioning devices was also a crucial concern. To ensure that the screen and honeycomb combination works as predicted, a gap of $\frac{2}{10}$ times the major dimension of the settling chamber is required between correction devices. The major dimension of the settling chamber was $12''$, making the required gap $2.4''$ between adjacent screens/honeycomb. The flow channel that was returned from the manufacturer had a $3''$ between screen flanges, which was more than sufficient to allow each to perform as expected.

A final requirement for the flow conditioning devices was that honeycomb requires a length 6-8 times the cell diameter of the honeycomb (Mehta & Bradshaw, 1979). The cell diameter of the

honeycomb was approximately 0.5″, which required the length of the honeycomb structure to be at least 4″. This requirement was easily satisfied since the length and width of the honeycomb structure were both 12″.

4.3 Fan and Motor Selection

The blade profile for the axial fan was chosen after first determining the exact dimensions of the inlet annular area of the flow channel, the desired flowrate, and the required static pressure rise across the fan.

The Work-Energy equation was applied with the assumption that the flow was incompressible, and then solved for the mechanical work required by the fan to produce a desired static pressure rise. The incompressible flow assumption was justified since the highest flow velocity produced within the channel was 55 mps or M = 0.162. From Bernoulli's equation, the required fan static pressure rise was determined to be equal and opposite to the static pressure drop expected through the screens and honeycombs. The Work-Energy equation was then formatted into Microsoft EXCEL, and expressed graphically as the motor power requirement for producing a given axial velocity in the test section [see Figure 9].
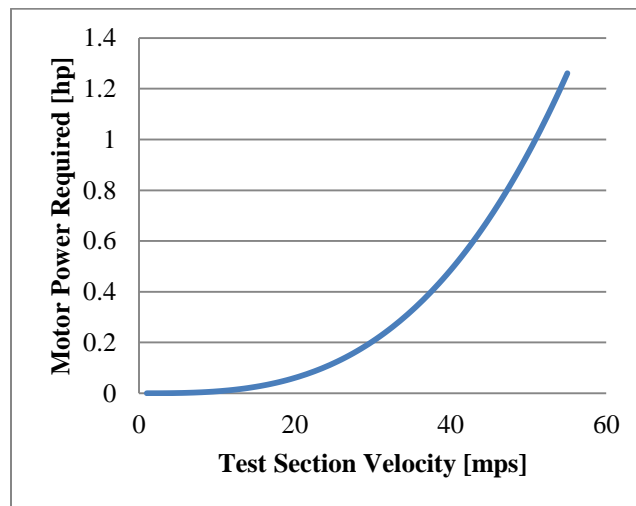
Figure 9: Power Curve for the Fan Motor

Note that the fan blades and drive system were assumed to be 100% efficient in this curve. The next section corrects for this poor assumption. Figure 9 shows, as expected, that the power requirement for the motor increases as the velocity produced in the test section increases, since more work is required from the shaft to turn the fan blades and produce this velocity. The maximum motor power requirement was extracted from this figure, by recording the motor power data point that corresponded to the maximum test section velocity. In order to produce an axial velocity of 55 m/s in the test section, it was found that 1.26 hp was required from the motor.

4.3.1 Axial Fan Selection

The next step in selecting the fan blade profile for the flow channel involved determining the blade efficiency through fan performance curves. Mehta and Bradshaw (1979) pointed out that fan blade efficiency and static pressure rise information is typically cataloged and provided by fan manufacturers.

After contacting several fan manufacturers, it was decided that Multi-Wing America would be the supplier of the projects fan blades. The reasoning behind this was that this company had a fan selection software program, which allowed users to customize a blade profile and hub configuration to meet desired operating requirements. The software inputs were: impeller diameter, operating RPM, static pressure rise, and flowrate.

Impeller diameter was chosen to be 11.8″, to minimize the fan blade tip clearance within the inlet annulus. Mass flowrate was chosen as 914 cfm, which corresponds to the upper limit if flow velocity in the test section. Static pressure rise required from the fan was set to be 7.8 inwg, which was approximately equivalent to the 7.63 inwg pressure drop across both the honeycomb

and screens. Operating RPM was not a fixed value, but rather it was varied to obtain a

performance curve that coincided with the other three values. Several iterations were run for the

operating conditions mentioned above, in order to find the blade profile with the highest

efficiency. The following performance curve was ultimately decided upon after consulting a

company sales engineer for a professional recommendation.
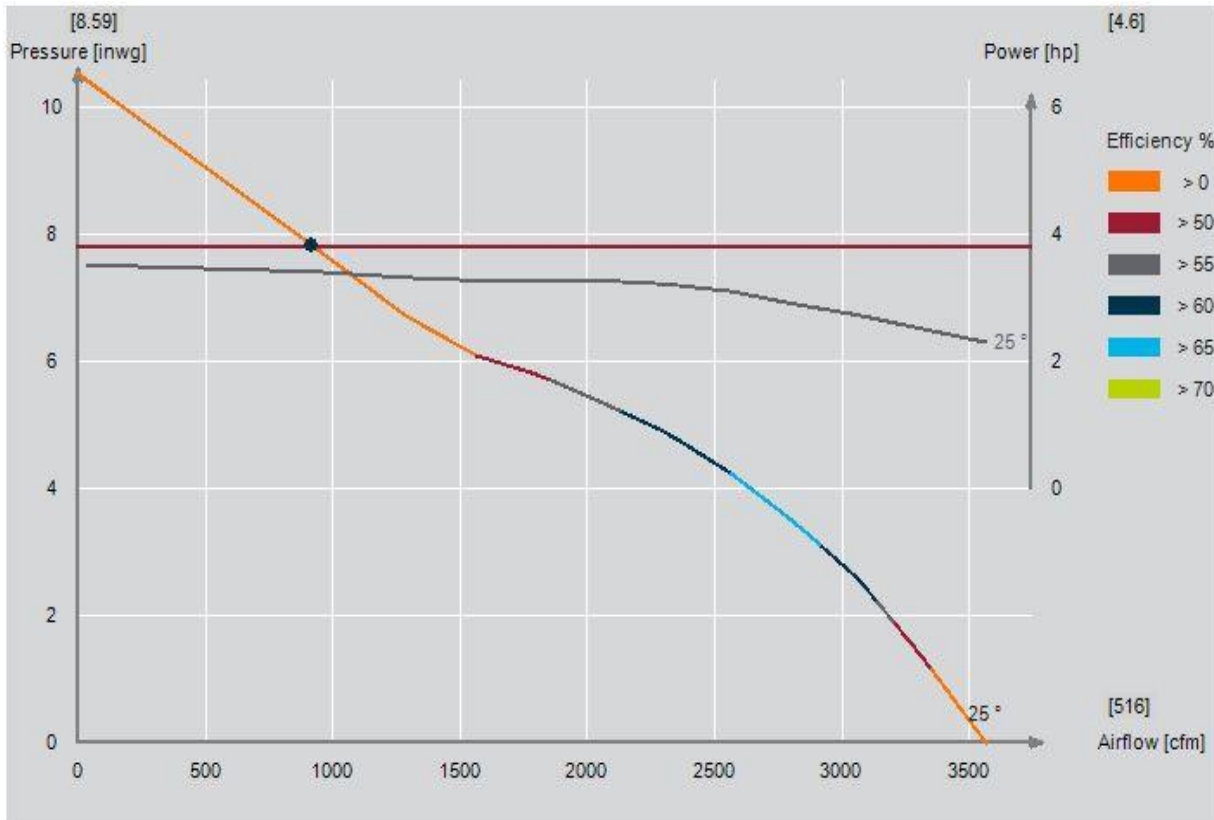
Figure 10: Fan Performance Curve (Multi-Wing, 2013)

The multi-colored curve in the figure above displays how the efficiency changes with the with

volume flowrate of air, for the chosen blade profile. This curve shows that the peak efficiency of

this blade falls between 2500 and 3000 cfm. The operational point of the blades however is at

914 cfm, and is shown by the intersection of the red and multi colored curves. The grey curve in

the figure above shows the power required by the motor to rotate the fan shaft at 6000 RPM.

The blade specifications from Figure 10 can be seen below in Table 1:

Impeller Parameter	Value
Impeller Diameter	11.8″
No of blades	6
Pitch	25 °
Blade Material	PAG
Air Velocity	6.12 mps
Airflow	914 cfm
Static Pressure	7.83 inwg
Speed	6000 RPM
Tip Clearance	0.5 %
Power	3.73 hp
Efficiency	33.75 %

Table 1: Impeller Information

This final fan blade efficiency was 33.75%, and the material chosen was glass reinforced

polyamide (PAG), for a test section velocity of 55 mps. Although another option was found with

a higher efficiency (36%), this option was decided upon since it produced a more uniform flow

distribution. A figure of the fan blade arrangement purchased is shown in Figure 11:

Figure 11: Multi-Wing Fan Blade Profile

4.3.2 Motor Selection

The selection of the axial fan provided two key parameters that were used to determine a suitable motor to power the system: the efficiency of the fan blades and the required RPM. Maximizing the fan blade efficiency minimized both motor cost and required hp. The motor power requirement of 3.73 hp was estimated after accounting for the efficiency of the fan in the preliminary work estimation. Note that this estimation neglects the efficiency of the motor itself as well the efficiency of the drive system, since this information could not be obtained from the companies from which they were purchased. A 3.8 hp Proform Power 990 Treadmill Drive motor was ultimately purchased for the drive system. This motor was purchased as a replacement piece, since it was listed at a more affordable price compared to that of competitors. The figure below shows this motor.

Figure 12: Proform Power 990 Treadmill Motor

This motor was tested using a prefabricated variable speed motor control board in the GTRL, and the operating RPM range was catalogued. The test revealed that the maximum attainable frequency from the motor was 30 Hz, which corresponded to a no load speed of 1800 rpm. Company policy prevented the treadmill manufacturer from providing the load performance

information to customers, therefore it was assumed for our fan drive system that the motor would maintain a similar RPM to that of the no load case.

4.3.3 Fan Drive System

From the previous section, it was apparent that the treadmill motor did not possess the necessary angular velocity to directly drive the fan at 6000 RPM. Because of this, a gear reduction ratio was applied between the motor shaft and the fan shaft to produce the desired angular velocity. A chain drive was chosen to drive the fan shaft over a belt drive, because it was the least expensive option out of the two options and it was far simpler to both fan and motor shafts. The figure below shows the setup for the fan drive system on the base of the rig. The larger of the two sprockets had diameter of 11.43″, and was attached to the motor face, while the smaller of the two had a 2.65″ outer diameter and was mounted to the fan shaft. The exact gear ratio for the system was then 4.31:1.
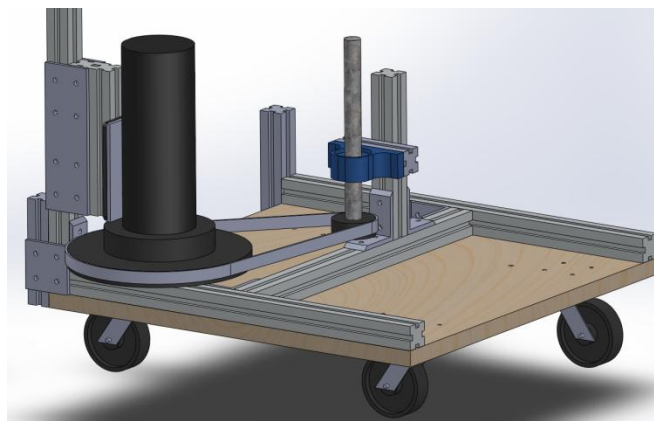
Figure 13: Fan Drive System

The fan shaft was positioned in the center of the base, and was attached to the base by a grease mounted bearing. The motor on the other hand was mounted to one of the vertical supports of the stand, by a reinforced aluminum plate.

4.4 Probe Manipulator

The final design of the probe manipulator was determined after the pros and cons were weighed for three different design configurations. Ultimately, a gimbal-type system was decided upon, but a traverse-driven system and a linkage system were also seriously considered.

4.4.1 Preliminary Designs

The preliminary traverse system design consisted of a semicircular arc with a small carriage-like piece that moved along the length of the arc, and was free to rotate at the pins holding the arc. The small carriage would have been connected to the probe holder, to allow for pitch variation along the semicircular arc. Figure 14 shows a Solidworks model of the proposed traverse system. The disadvantage of this design was that it would have been costly since it required an exact semicircle for the arc component. Any deviation from circular would provide inaccuracies in the probe head location. The benefit to having this type of device would have been the capability of traversing a full 180 degrees in both pitch and yaw.

Figure 14: Traverse System Design

Several methods were considered for driving the carriage along the semicircular arc. One method involved using a tape drive to push and pull the carriage along the track al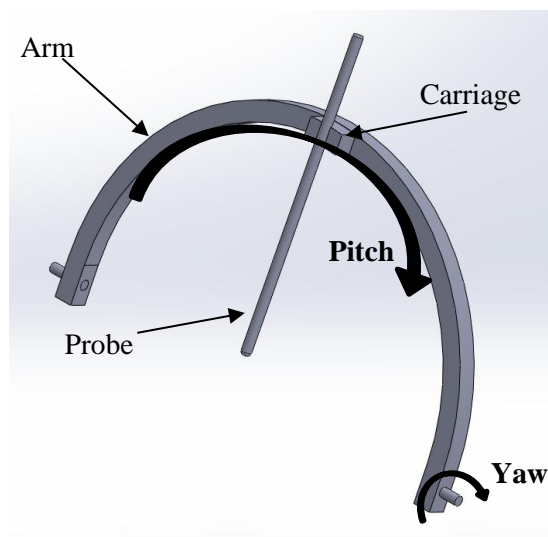ong the arc. This system would have been simple and easy to construct, however it would have been limited in accuracy due to slippage and stretching of the tape. The tape drive would have needed to fit into a track itself, which would have necessitated small movements, which would have led to inaccuracies.

Instead of a tape drive, another idea was to use a system of weights and pulleys to drive the traverse. In this system, a string connected to a motor would have needed to be attached to a freely hanging weight along the side of the test section of the flow channel. There were several connection concerns with this system, but the main reason why this system wasn't selected was because it would have been unstable when exposed to the drag force of the flow coming from the test section.

 A third idea was to use a 4 bar linkage to pitch the carriage system across the semicircular arc. For this hypothetical system, two sets of parallel bars would have been connected to one another as shown in Figure 15. Point C on the figure would have been attached to the carriage-traverse, and point D would have needed to be the fixed pivotal point, positioned at the center of the arc. Driving this system would have been complicated, since it would have relied on translational rather than rotational motion, and inaccurate because there would be losses associated with each linkage and hinge.
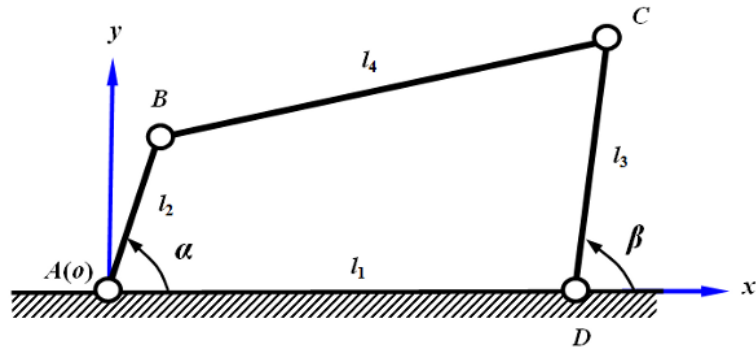
Figure 15: 4 Bar Linkage (Jing-Shan Zhao, 2008)

4.4.2 Final Design

A final approach chose was to create a gimbaled device. The first iteration of this device consisted of two L-shaped arms attached to each other with a fixed axis for the probe to attach to the end of one of the arms. With this design, the tip of the probe will not translate at all, no matter how the arms are rotated, as displayed in Figure 16.
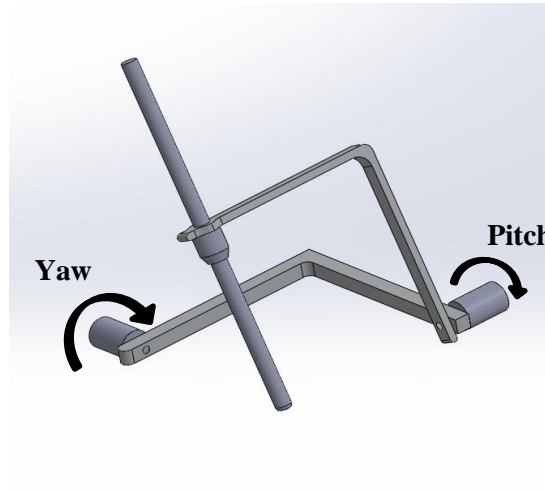
Figure 16: General Probe Holder Design

Stepper motors were originally chosen to provide the pitch and yawing motion, and are shown as cylinders in the figure above. The openness of this design was its greatest feature, and meant that it could achieve a wide range in motion. This feature also meant that the yawing stepper motor would need to possess a larger torque output to handle the loading of the entire system. The

loading on each of the two arms would also be considerable, and deflections would be a serious concern.

This design allows for many slight alterations to better achieve the 180 degrees of pitch and yaw objectives. Rectangular arms were used in this design instead of the semicircular arms of the traverse design because they accomplish the same angular variation, and are much simpler to construct. A stress calculation were carried out to see if this design was feasible, and resulted in the failure of one of the two arms. The design was then slightly modified to better distribute the loading on each of the arms. Figure 17 below shows the modified design.
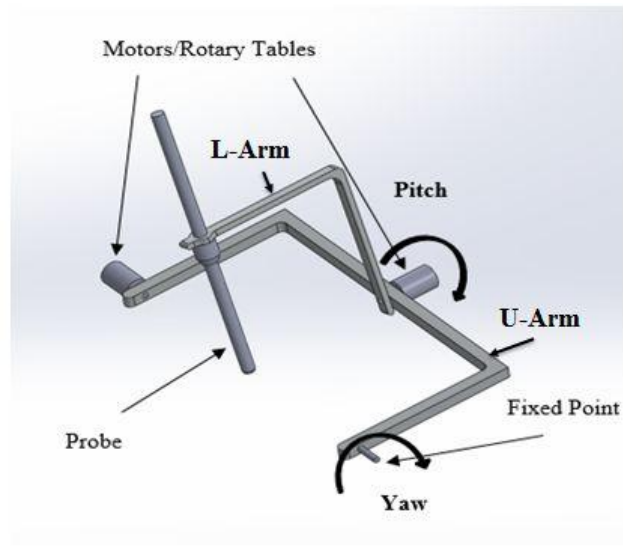
Figure 17: Modified Gimbal with U Shaped Arm

A finite element stress simulation was conducted in Solidworks to determine what dimensions for the U and L shaped arms would produce an acceptably small deflection for the various loads that each bar was subject to. These loads included that from rotational devices, the probe holder, the distributed loads from each arm, and the also the drag force from the airflow. The thicknesses and lengths of the U and L shaped arms were varied until the deflection was less than .1mm for each arm. Figure 18 below shows the results of the deflection simulation.
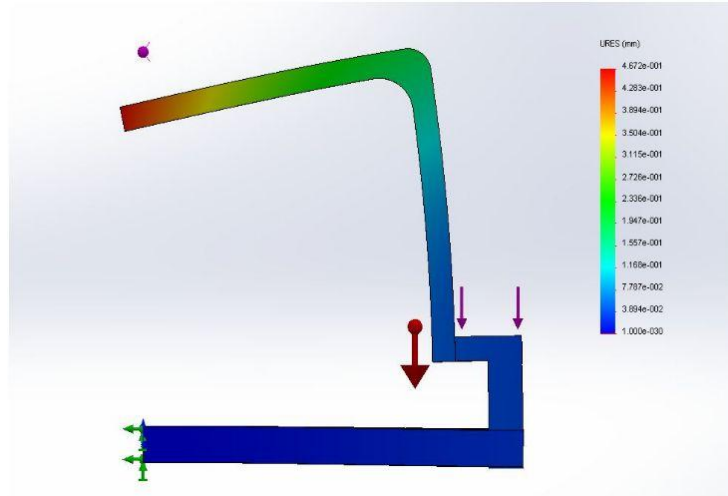
Figure 18: Solidworks Stress Analysis

The simulation yielded a negligible deflection for a U shaped arm with a .75″ square cross section, with a midsection length of 14.25″, and two side lengths of 9.25″, and a deflection of less than 0.1mm for the L shaped arm, with a .5″ square cross section, a side length of 7.5″, and a length of 6″ on the other side. The material chosen for the arms was aluminum 6061, because it was both lightweight and inexpensive. The color legend on the side of Figure 18 shows the range in deflection from largest (red) to smallest (blue). It is important to note also that the deflection shown in the figure above is an exaggeration of the actual deflection.

After it was decided that this design would be used, the next issue was determining how to rotate the two arms. Two off-the-shelf options included rotary tables and stepper motors. Stepper motors were originally going to be used, but after the tolerances for each of the two options were compared, rotary tables were chosen. The cost of these devices was significantly higher, but these devices were capable of accuracies to within $\frac{1}{10}$ degree. The rotary tables were purchased from Velmex Inc. because they were the most affordable option, and also because the GTRL already had a Velmex 3-axis linear traverse controller, which could also be used to control the

rotary table movement. The maximum torque for the larger of the two rotary tables was 3.75 ft-lb, and the smaller of the two was 1.25 ft-lb, which was sufficient to support the applied loads acting on each of these devices.

In order to connect the rotary tables to the arms of the probe manipulator, two intermediary plates were designed. These two plates were made out from aluminum, and were designed to be screwed into both the rotating faces of the rotary tables and the ends of the L and U shaped arms.

The next step in the design process was determining where the rotary tables would be connected in relation to one another. The one major constraint on the location of the two rotary tables was that the pressure probe head or velocity probe head needed to be aligned with the axes of both rotary tables. This constraint allowed the probe head to remain in a fixed position regardless of any angular position of either rotary table.

The objective of the project was to develop a probe manipulator with pitch and yaw ranges of 180 degrees. However, after taking into account the stress limitations on each of the manipulator arms this objective became unachievable. Rather than achieving 180 degree ranges of pitch and yaw, the new objective became maximizing the achievable ranges of both rotary tables by choosing optimal positions for each of these devices. The optimal position for the smaller of the two rotary tables was 3″ from the inside corner of the U shaped arm. The optimal position for the larger rotary table had the U shaped arm offset 1.65″ from this rotary tables' axis. This position yielded a pitch angular range of 158 degrees, and a yaw angular range of 170 degrees. A Solidworks model of this offset design is shown in the following figure:
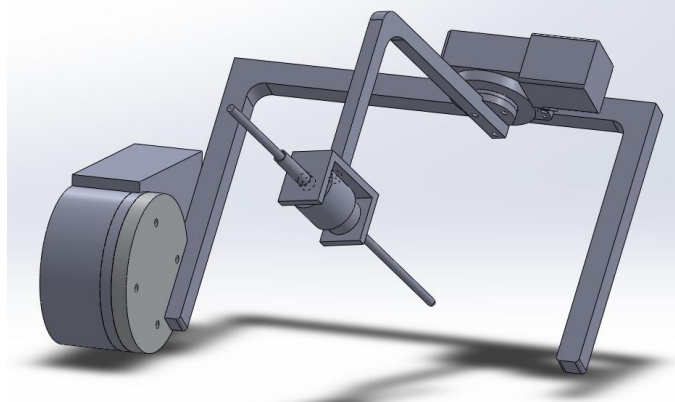
Figure 19: Offset Probe Manipulator

4.4.3 Probe Holder

The final component to the probe manipulator design was the probe holder. This component had to be able to hold different size probes without damaging them, it had to be able to hold probes in a solitary position, and it also needed to be supported by the L shaped probe manipulator arm. To satisfy these requirements, a four piece assembly was constructed. The assembly components consisted of a drill chuck, a hollowed out threaded rod, a two pronged connection block, and a thin cylindrical tube for securing the hot wire probe. The drill chuck was the key component in this assembly, since it was adjustable to allow for different sized probes, provided a way to regulate how tightly the probes were held, and also made sure that probes would always be held along the axis of the chuck.

A bolt connection was used to fasten the connection block supporting the drill chuck to the L shaped arm. The thread mount on the inside of the drill chuck was then used to attach the chuck to the two pronged connection block via the hollow threaded rod. The last piece of the assembly, the cylindrical probe holder tube was lastly inserted through the threaded rod and chuck. Figure 20 below provides a good illustration of this assembly.
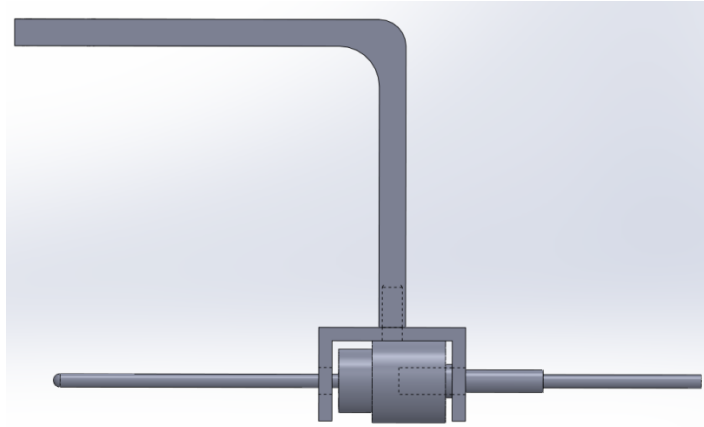
Figure 20: Probe Holder Model

4.5 Stand Design

The stand design was influenced by the designs of the flow channel, probe manipulator, and the

fan drive system. The first function of the stand was to house each of the components listed

above. However, the stand needed to be adjustable, so that the probe manipulator could be easily

aligned with the test section of the flow channel. Furthermore, the rig as a whole needed to be

maneuverable to move from the GTRL to the Fluids research lab in the basement of Higgins

Labs. Since probe calibration requires both high accuracy and precision, additional care was

taken to eliminate any vibrations that were likely to have been created by the fan blades or the

motor.

Cost was one of the larger drivers in the decision to go with a plywood base for the stand, since

this material was readily available, for little to no out of pocket expense. 80/20 framing material

was the other resource that was in large supply around the GTRL, which was again the

motivation behind the design. The 80/20 material was an ideal choice for the frame of the rig,

since it provided a rigid connection, but was also easily adjustable for probe manipulator

positioning. The plywood base of the stand needed to be sufficiently large to fit the flow channel

within it. Since the bell mouth on the flow channel was 21″x21″, the plywood base was chosen

to be 26″ x 30″, allowing the channel to be removable from the stand if need be without disassembling the entire structure. The larger size, also allowed the casters on the bottom of the rig to be dispersed more evenly to share the unevenly distributed load of the rig, and it also allowed for room to be included for the expanded metal-filter component to fit within the base of the rig. It was crucial to include the filter into the stand design, because it acted as a dust and dirt collector, which helped to keep the flow through the channel clean. Casters, on the other hand, satisfied the portability objective for the channel, and anti-vibration mounts were attached in addition to the casters, for the ability to level the rig and account for the unevenness of the floors in the GTRL.

The frame design consisted of four vertical members reinforced along the edges of the base and connected by four more horizontal beams in the same plane towards the top to support the flow channel. Built up off of the support plane at the top are two L-shaped structures with attachments for the rotary tables, as shown in Figure 21. This design is especially beneficial for two reasons. First, it allows the various types of probes to be aligned precisely with the top of the test section. Secondly, it allows the weight of the upper part of the rig to be carried on the two cross beams, improving structural stability and reducing unwanted swaying or wobbling that could affect the accuracy of the calibration process.
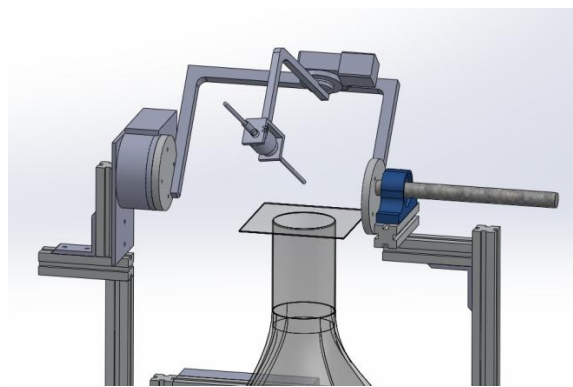
Figure 21: Probe Manipulator Mount

Figure 22 below shows the Solidworks model of the final velocity probe calibration rig design. Note form the figure that the flow channel is shown as a transparent object, the reason for this was so that the fan drive system could also be visible beneath the channel. The probe manipulator can be seen clearly at the top of the structure. Two electronic power boards were added to the model to show where the rotary table controllers and motor controllers fit into the design.
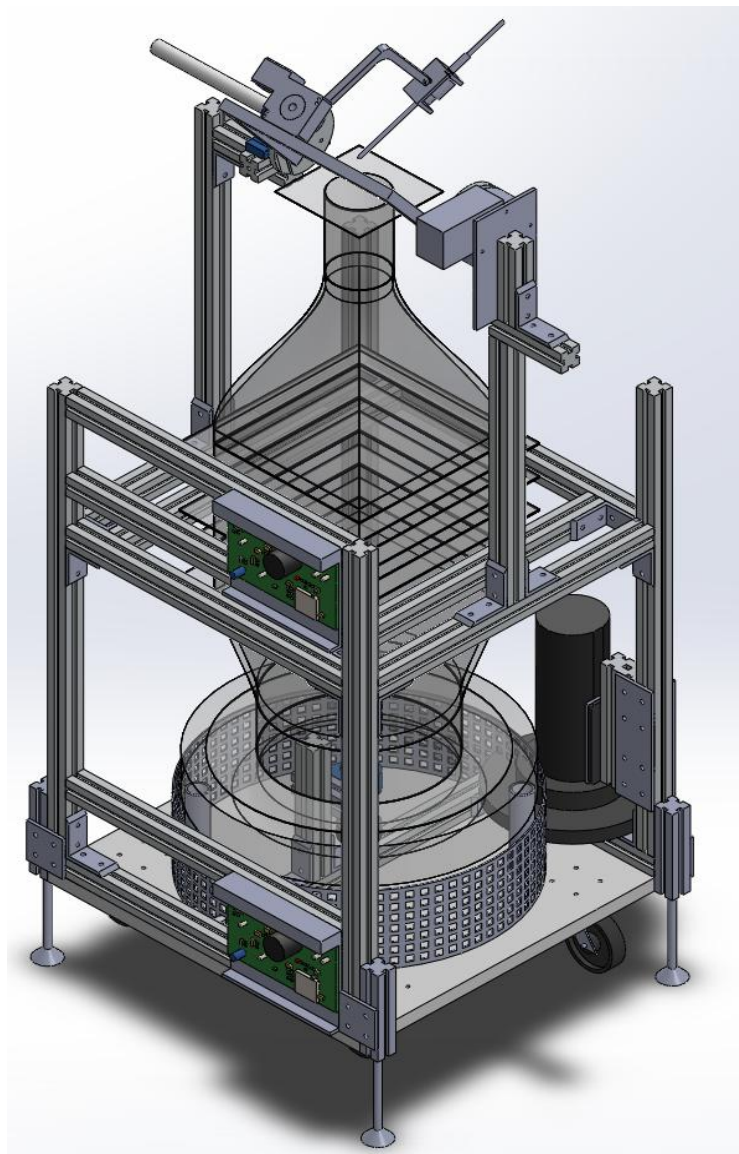
Figure 22: Final Velocity Probe Calibration Rig Design

4.6 Motor Controller Design

The most effective motor controllers use pulse width modulation (PWM) to provide power to the motor. The easiest and most cost effective way to control the motor was to use the control board designed for the motor and a pulse width modulation circuit. The controller operates by converting the DC signal it receives to a strength that the motor can use. To provide a useful input signal a simple pulse width modulation circuit was built with a potentiometer to control the pulse ratio.

5 Construction

The manufacturing of the rig can be broken down into four main sections. The first section describes the manufacturing of the flow channel, the second covers the construction of the stand for the rig, the third discusses the system created to drive the fan, and the final section details the build of the probe manipulator. Several compromises were made in the manufacture of components because of machining limitations. The bases for any deviations from design were explained in the following sections.

5.1 Flow Channel

A flow channel was manufactured by Gray Metal Products which included a test section, a contraction section, a settling chamber, and a diffuser section. The channel was manufactured as a single piece of sheet metal, instead of five separate components that would attach together, and was also missing an inlet and bell mouth section. Several modifications were made to the original piece, to create a better replica of the finalized design structure. These modifications included: cutting the settling chamber into three pieces, adding flanged sections to the cut pieces, bending a thin sheet of aluminum into a cylindrical inlet, adding a flange onto the aluminum inlet, and tapering the test section to create a smooth outlet.

Pop rivets were used for connections of the flanged sections for both the aluminum and sheet metal pieces, because welding would have compromised the structure of either material. After the flanges were secured onto each settling chamber piece, an industrial sealant was used to bond the flanges to the screens. To reinforce these connections, three nut and bolt connections were added to the each side of the flange. Smoothing off the test section required tapering the small lip at the exit of this section with a mallet and several clamps. Figure 23 below shows the flow

channel after the final stages of construction, before the addition of the screens, honeycombs, and bell mouth section.

Figure 23: Assembled Flow Channel

Spare tooling board in the GTRL was used to make the bell mouth section for the flow channel. First the board was cut into a square 24″ by 24″ section with a 3″ depth, and then the piece was taken to the VM3 CNC in Washburn Shops to cut out the precise shape from the Solidworks model that was developed. Cutting the tooling board with this machine was a tedious process, because the machine needed to be cleaned repeatedly to prevent a harmful reaction between the ventilation coolant and the dust particles created from the cutting process. The machine shop manager instructed the team to cover the machine's sliding weights, metal chip remover, and coolant vents with a plastic wrapping in order to prevent this harmful reaction. The figure below shows the tooling board piece within VM3 CNC machine after the 12″ pocket on the inside had been milled out.

Figure 24: VM3 CNC with Tooling Board Bell Mouth

The final length and width dimensions for the tooling board piece were 21″x21″, with a 3 in depth. Four ½" clearance holes were added to the tooling board piece for the risers for anchoring the flow channel to the stand.

5.2 Stand

The stand was a very straightforward structure to construct, since it was made up of a plywood base, casters, risers, and an 80/20 frame. The dimensions for the Solidworks model presented in section 4.5 were followed directly. The 80/20 pieces and the plywood piece were cut with a vertical band saw and then sanded to within a tolerance of $\frac{1}{8}''$ with a belt sander. The 80/20 pieces were bracketed together to ensure that the frame was rigid, and the casters were screwed into the plywood piece from the underside with wood screws. Anti-vibration mounts were purchased from Air Inc. to serve as risers for the stand, in order to dissolve any vibrations transferred from the fan or motor to the rig's surroundings.

5.3 Fan Drive System

Driving the fan with the treadmill motor via the system described in section 4.3.3, first required

drilling and tapping holes into the treadmill motor face. A precise hole pattern was drilled

through the face of the motor using a CNC machine and was later tapped with a $\frac{5}{16}''$-24 thread.

An identical pattern was later created on 11.43″ OD sprocket used in this system by following

the same process. Figure 25 below shows the sprocket on the CNC machine in the Higgins

Machine Shop. The sprocket was then mounted on the motor face and the two components were

joined together with a $\frac{5}{16}''$-24 bolt and finally mounted back onto the body of the motor.

Figure 25: Motor Sprocket on the CNC machine

The next step in constructing the fan drive system was to assemble the mount for the fan shaft.

This subsystem consisted of a grease mounted bearing, the fan drive shaft, bushing, and the 2.65″

OD sprocket. The quick disconnect bushing locked into place on the fan shaft after being

tightened with a vice. Threaded screws were aligned with the sprocket on the end of the fan shaft, and the sprocket was hammered into position. The inside diameter of the bushing had originally matched the outer diameter of the bar, but with the sprocket squeezing on the outside of the bushing, the inside diameter of the bushing decreased slightly. The rod-bushing-sprocket was then inserted into the grease-fitted mounted bearing and the eccentric lock nut was tightened around the rod to keep it in place. The figure below shows the connection of all the discussed pieces.

Figure 26: Sprocket for Fan Shaft

To complete the assembly, the fan blades purchased from Multi-wing were mounted to the top of the fan shaft using the screw connections built into the fan hub.

5.4 Probe Manipulator

The manufacture of the probe manipulator required a high degree of precision to ensure that the tip of the probe head would be aligned exactly with both rotary tables' axes. After consulting with the head machinist in the Higgins Laboratory machine shop, it was decided that the best

way to manufacture the U and L shaped probe manipulator arms was to create an assembly of smaller components, rather than cut singular pieces with a CNC machine. This process deviated from the original design process slightly, but produced an identical result to that of the original design idea.

The new U shaped probe manipulator arm was composed of 3 bars, each with a .75″ square cross section. The length of one of the bars was 14.25″, whereas the lengths of the other two were 9.25″. The new L shaped arm was made up of two bars with .5″ square cross sections. The lengths of these bars were 6″ and 7.25″. Connecting each of these pieces together required 4-hole corner bracket pieces, which were individually fabricated from aluminum 7075 plates using the CNC in the Higgins Machine Shop. Figure 27 below shows the bracket connections being cut on the CNC machine.
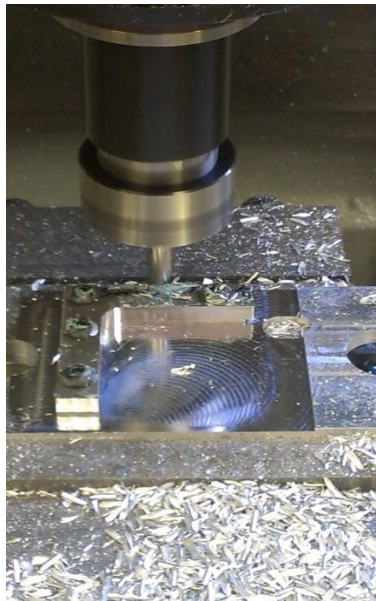

Figure 27: Probe Manipulator Brackets

After the brackets were fabricated, the U and L shaped arms of the probe manipulator had holes drilled in identical locations as those on the corner brackets. These holes were then tapped with a

$\frac{1}{4}''$-20 tapping tool, to allow for a bolt connection on either side of the arms. $\frac{1}{4}''$-20 bolt connections were then used to assemble all of the discussed components.

Due to time constraints, the manufacture of the probe manipulator was unable to be fully completed. The next pieces to be machined were the intermediary connection plates described in section 4.4.2. These pieces needed to be cut on the CNC machine, since they were supposed to tightly adhere to the probe manipulator arms, but they also required a precise hole pattern for mounting to each of the rotary tables.

The final pieces to be machined for the probe manipulator were those pertaining to the probe holder. Leftover $\frac{1}{2}''$-13 threaded rod from the stand risers was ultimately going to be fit into the probe holder piece, and hollowed out with a $\frac{5}{16}''$ clearance hole drill bit, so that this piece could then hold both the pressure and hot wire probes. The final tasks for the probe manipulator consisted of widening the chuck holder pocket with a manual milling machine, and then fitting this piece with the $\frac{1}{2}''$-13 hollowed out threaded rod, and lastly manufacturing a $9''$ cylindrical tube ($\frac{5}{16}''$ OD, $\frac{1}{4}''$ ID) with a wing nut connection on one end for holding hot wire probes within the chuck holder.

6 Rotary Table Control

Control of the rotary tables for the probe manipulator was accomplished by developing a LabView program which sends commands to the rotary table stepper motors through a user interface. This program runs as a step-by-step process beginning by establishing a connection with the stepper motor, which allows for back and forth communication between the stepper motor, and the stepper motor controller. The next step of the process involved specifying a starting position for the rotary tables. After these steps were said and done, the rotary tables then process the user inputted information, and complete the user specified trajectories.

By accepting the connection from the stepper motor controller, the stepper motor engages itself into the 'online' control mode, which then allows the motor controller to read and respond to the commands from the LabView user interface. After this basic setup, a set of commands is sent to the stepper motor controller, ensuring that various parameters are properly recognized. These parameters include motor type, limit switch operating mode, rotational speed, and initial positioning. Note that the limit switch operating mode involves setting the limit switch to allow a home position for the motor, and initial positioning ensures that the motor has moved to this home position. Motor type and rotational speed are self-explanatory, preset parameters, which can be located from the rotary table specifications. After this point, the rotary tables should be prepped and ready to accept user inputs.

After the inputs are provided by the user, the validity of each of the values is checked. If one of the numerical values is determined to be invalid, then an error message will appear on the screen and the program will not run. If there are no error messages, then the user is provided the option

of using the even intervals switch. The figure below shows the block diagram of the user interface, complete with all inputs, and available options.
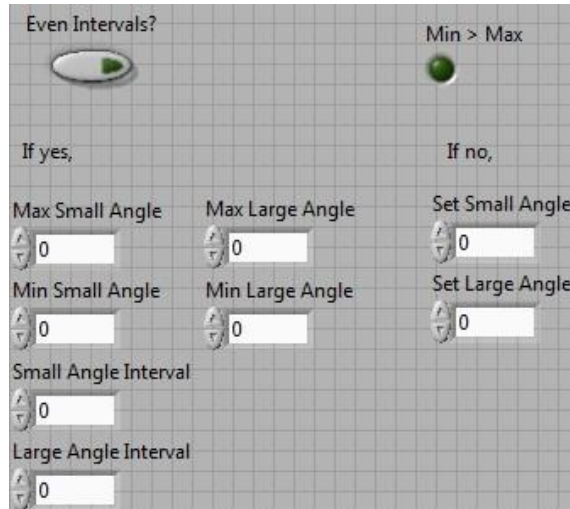

Figure 28: LabView User Interface

The small angle inputs refer to the angles of the smaller of the two rotary tables, whereas the large angle option refers to the larger of the two rotary tables. The maximum and minimum angles on the user interface allow for the range to be specified for each rotary table, and the interval option specifies the number of degrees each rotation will provide to its respective motor. The set angle input on the other hand fixes each rotary table to a certain position. Between increments, there is a 1.5 second pause, which allows measurement data to be collected. After the measurement process is complete, the motors return to their home position, the stepper motor controller closes its connection to LabView and vice versa, and finally the debug menu is closed.

There are few other safety factors, aside from the (Min > Max) LED, built in to the program to limit the range of the testing equipment, and otherwise prevent the damaging of testing equipment. For example, the number of measurement points is also rounded down to prevent motion from exceeding these limitations. Negative inputs are automatically converted to positive

values, to ensure that the rotary tables only function within at most a 180 degree plane. Lastly, and most importantly, ±90 degrees was set as the absolute maximum range that each rotary table can turn.

6.2 Testing Procedures

The first step in the operation of the rotary tables is ensuring that all limit switches are connected to the stepper motor controller, and that the controller is plugged in to an electrical outlet. After ensuring these basic connections are made, the stepper motor controller can be turned on, and the startup procedures can commence. By running the Initialize.vi program, the stepper motors will be configured to their home positions or adjusted to a new home position of the user's choice.

The Rotary Motion.vi file can then be launched, which should provide the user with access to the User Interface block diagram. Here the user can input the pitch and yaw ranges for each of the rotary tables, as well as the interval over which the measurements are taken. Ranges exceeding ±90 degrees, or improper inputs will yield an error message, in the form of an LED, and the commands will not activate. Selecting the even intervals switch on the user interface will allow for multiple measurements to be taken with a uniform measurement interval.

When finished collecting measurement, make sure the 'online' light on the front display of the stepper motor controller is off. If it is still on, running the Initialize.vi program should resolve this issue, otherwise the user should consult the Troubleshooting section of the Vxm User Manual. The stepper motor controller can then be turned off and disconnected from both the computer and power outlet.

7 Conclusion

A velocity probe calibration rig was designed for fluids research at Worcester Polytechnic Institute. Several different iterations were considered before a final model was chosen and drafted in Solidworks. The final design consisted of several key components, including a probe manipulator with two rotational degrees of freedom, a blower-type flow channel with an axial flow fan, and a drive shaft system powered by a treadmill motor. The probe manipulator was designed for a ±79 degree range in pitch, a ±85 degree range in yaw, and a $\frac{1}{10}$ degree turning accuracy. It was also designed to be compatible with both pressure and hot wire probes. The achieved ranges in pitch and yaw were on par with the ranges of other devices described in the literature, but were slightly below the ±90 degrees described in the project objectives. The drive system for the axial flow fan was designed with the ability to produce a test section flow velocity of 55 mps, which satisfied the maximum flow velocity objective for the rig.

The construction of the flow channel, the fan drive system, and the stand were completed by the project deadline. The probe manipulator, on the other hand, was not able to be completed within this timeline. The flow channel was first manufactured by a ducting company, Gray Metal Products Inc., and then later modified to meet all of the requirements of the design model. The drive shaft system for the axial fan was constructed and successfully tested with a preexisting motor controller circuit. A separate, variable speed motor controller circuit was constructed for the treadmill motor, but proved unable to power the system. An adjustable stand was manufactured from 80/20 framing material that was both rigid and maneuverable. Despite not fully finishing the probe manipulator component, a LabView program was created and tested for

controlling the rotary tables of the probe manipulator. The test was successful, and allowed users

to designate an operational range and incremental interval for flow measurement.

8 Recommendations

8.1 Screen Maintenance

Pope and Rae (1984) recommend that wind tunnel screens are cleaned every 5 years. With this requirement in mind, three flanged sections were included in the design of the flow channel of the rig, to allow for easy access to the screens for cleaning purposes. The flanged sections were bonded to the screens in the settling chamber with an industrial sealant, to ensure that airflow would not escape the flow channel and that the connection would be secure. The channel developed for this project was vertically oriented with the inlet within one foot of the floor. Because of this orientation, there was a higher risk that dust and dirt would accumulate within the screens. It is recommended that the screens therefore be cleaned on a 2-3 year basis, and the sealant be replaced, to ensure that flow through the flow channel remains both clean and uniform.

8.2 Vibration Damping

Due to constraints in time, anti-vibration mats were not included in the design or the build of the rig. It is important to include these components into the rig, to reduce the transmission of the vibrations from the motor and fan blades to the probe manipulator. The anti-vibration mats should be located between the fan and motor components and the 80/20 frame to effectively isolate these components. Further research should be done to determine a material capable of eliminating all vibrations generated from each of the two sources.

8.3 Tolerances

All of the mechanical connections and machined components included in the rig have individual tolerances, which are measures of the deviation from the design specifications. The error within each of the rig components subtracts from the absolute positioning accuracy of the probe head within the flow channel test section. To lower the tolerances within the frame, it is recommended that all 80/20 pieces be re-trimmed to more precise lengths with one of the manual milling machines located in the Higgins Laboratory machine shop. The tolerances provided by the manual milling and CNC machines, should be available on the machinery specifications. After determining all tolerances throughout the rig, the precision error can be calculated and then quoted as the achievable accuracy for the rig.

Alignment of the rig is the other important concern with testing accuracy. Perfect alignment of all components is an unrealistic expectation for the rig, since it will be frequently transported between fluids research labs at WPI. To ensure quality alignment of the rig, it is recommended that a level be used to reduce unevenness at the base of the rig structure.

8.4 Probe Head Alignment System

Due to time constraints, this project was unable to produce a system for aligning the probe head with respect to the center of the flow channel test section. The function of the rotary tables was to rotate the probe head about two sets of axes, but the probe manipulator system designed and constructed for this project fails to address how the probe head would be aligned with respect to the test section center. Holding the probes was accomplished using a drill chuck, but this system doesn't have any way of discretizing the translation of the probe along the axis of the chuck. In the future, a system should be implemented to accomplish this task.

8.5 Rotary Table Control

Future progress on the rotary table control should edit the LabView code to include a negative angle interval to allow the position iterations to begin at the minimum applicable angle, and increase incrementally toward the maximum. Incorporating this feature into the LabView program would ensure that the rotary tables do not attempt to intersect with the probe manipulator arms, and otherwise damage the probes.

8.6 Closed Loop Motor Controller

This project was unsuccessful in developing a control system for the treadmill motor that was purchased. A pulse width modulation control system was constructed, but was unable to vary the speed of the motor, or for that matter even power the motor. It is recommended that those continuing with this project pursue a motor controller design with a closed loop feedback system formatted in LabView.

8.7 Fan RPM Measurement

In the future, we recommend including a device to measure the exact RPM at which the fan is running at. One potential system would employ a light sensor and a digital readout display, where the sensor would be attached directly to the inlet annulus, and would record angular rate as a function of signal disturbances. This system was successfully employed by (Baiense et al. 2012), where a light sensor was used to measure the RPM of a motor driving a moving bar wake generator around a linear cascade.

8.8 Probe Manipulator Construction

Before the project deadline, the probe manipulator arms were fully manufactured along with the connection bracket pieces, however the probe holder piece and the rotary table plate connections still required some construction. First off, the pocket inside of the chuck holder needed to be widened with a manual milling machine, and then fitted with the $\frac{1}{2}''$-13 threaded tube. After that, the hot wire probe required a $9''$ cylindrical tube ($\frac{5}{16}''$ OD, $\frac{1}{4}''$ ID) with a wing nut connection on one end to allow it to be held within the chuck holder. The three rotary table plate connections on the other hand simply required some milling in the CNC machine, which should be very straightforward, since models of these pieces have already been created in Solidworks. The very last task with the probe manipulator, would be to assemble all of the pieces according to the model created in section 4.4.

References

Aeroprobe Corporation. (2012). "Aeroprobe Conventional Multi 5- and 7- Hole Probes".
    Retrieved October 2012, from Aeroprobe:
    http://www.aeroprobe.com/probes/view/conventional-multi-hole-probes

Amgad, E. D. (2002). "Performance Analysis of Axial Fans in Unitary Air-Conditioning
    Systems". *Hammond: Purdue University Calumet*. West Lafayette, Indiana.

Baiense, J., Chichester, F., Egan, M., Madamba, S., Moore, S., & Wakeman, J. (2012). "Design
    of Moving Bar Wake Generator for a Linear Compressor Cascade". Major Qualifying
    Project. Worcester Polytechnic Institute.

Bruun, H. H. (1995). "Hot-Wire Anemometry: Priciples and Signal Analysis". *Oxford.* New
    York, New York, United States of America.

Comte-Bellot, G. (1976, January). "Hot-Wire Anemometry". *Annual Review of Fluid Mechanics,
    8*, 209-231.

Dantec Dynamics. (n.d.). "Hot-wire anemometry, Constant Temperature Anemometry".
    Retrieved September 27, 2012, from Dantec Dynamics:
    http://www.dantecdynamics.com/Default.aspx?ID=654

Díaz, A. K., Oro, F. J., & Blanco, M. E. (2008). "Cylindrical three-hole pressure probe
    calibration for large angular range". Gijón, Spain: *Flow Measurement and
    Instrumentation*.

Dixon, S. L., Hall, C. A. (2010). "Fluid Mechanics and Thermodynamics of Turbomachinery".
    Oxford, UK: Elsevier Inc.

Dominy, R. G., & Hodson, H. P. (1993). "An Investigation of Factors Affecting the Calibration
    of Five-Hole Probes for Three-Dimensional Measurements". *Journal of Turbomachinery*,
    513-519.

Doolan, C. J. (2007). "Numerical Evaluation of Contemporary Low Speed Wind Tunnel
    Contraction Designs". *The Journal of Fluids Engineering*, 1241-1244.

GUO, H. M. (2007, September 24). "Effects of a Kind of Non-smooth Blade on the Unsteady
    Flow Field at the Exit of an Axial Fan". *Journal of Thermal Science, 17*(1), 1-6.

Hu, F. T., & Hsu, Y. Y. (1994). "A probe manipulator for wind tunnel experiments". Taipei,
    Taiwan: *National Taiwan Institute of Technology*.

Jing-Shan Zhao, F. L.-J. (2008). "Mobility of Spatial Parallel Manipulators". Beijing: *Tsinghua University*.

Li Zhang, Y. J. (2011). "Effect of Blade Numbers on the Performance and Noise of small Axial Flow Fans". Hangzhou: *Trans Tech Publications*.

McMaster-Carr. (2013, February 22). Retrieved from McMaster-Carr Web Site: http://www.mcmaster.com/

Mehta, R. D., & Bradshaw, P. (1979, November). "Design rules for small low speed wind tunnels". *The Aeronautical Journal of the Royal Aeronautical Society*, 443-449.

Michael J. Martin, K. J. (2006). "Design of a Low-Turbulence, Low-Pressure Wind-Tunnel for Micro Aerodynamics". *Journal of Fluids Engineering*, 1045-1051.

Morrison, G. L., Schobeiri, M. T., & Pappu, K. R. (1998). "Five-Hole Pressure Probe Analysis Technique". *Flow Measurement and Instrumentation 9*, 153-158.

Omega Engineering. (n.d.). "Stepper Motors". Retrieved September 20, 2012, from www.omega.com: http://www.omega.com/prodinfo/stepper_motors.html

Ostowari, C., & Wentz Jr., W. H. (1983). "Modified Calibration Technique of a Five-Hole Probe for High Flow Angles". *Experiments in Fluids*, 166-168.

Pankhurst, R., & Holder, D. (1952). "Wind-Tunnel Technique". Bath, Great Britain: Sir Issac Pitman & Sons, Ltd.

Paul, A. R., Upadhyay, R. R., & Jain, A. (2011). "A Novel Calibration Algorithm for Five-Hole Pressure Probe". *International Journal of Engineering, Science and Technology Vol. 3 No. 2*, 89-95.

Pittoni, M. (1989). "The Breda Wind Tunnel". Washington: *National Adisory Committee for Aeronautics*.

Pope, A., & Rae, W. H. (1984). *Low-Speed Wind Tunnel Testing* (2nd Ed. ed.). New York: *Wiley*.

Ramachandran, N., Smith, A., Gerry, G., & Kauffman, W. (1995). "High Reynolds Number Effects on Multi-Hole Probes and Hot Wire Anemometers". Redstone Arsenal: *NASA*.

Roshdy, Kareem. (2013). "30 in. x 30in. Blower Tunnel". Retrieved February 20 from ZE-Engineer: http://ze-engineer.blogspot.com/2011/06/wind-tunnel-basic-types.html.

S. M. Gorlin, I. I. (1964). "Wind Tunnels and their Instrumentation". Jerusalem: Isreal Program for Scientific Translations.

Santiago Pezzotti, J. I.-m. (2009). "A Wind Tunnel for anemometer calibration in the range of .2-1.25 m/s". *Elsevier*, 338-340.

Scheiman, J., Marple, C., & Vann, S. D. (1982). "A Calibration Technique for a Hot-Wire-Probe Vector Anemometer". *NASA*.

Smith, J. R. (2005). "Programming the PIC Microcontroller with MBasic". Oxford, United Kingdoms: *Newnes*.

Thomas J. Benson, C. A. (2010). "The Beginner's Guide to Wind Tunnels with TunnelSim and TunnelSys". Orlando: *National Aeronautics and Space Administration*.

Treaster, A. L., & Yocum, A. M. (1978). "The Calibration and Application of Five-Hole Probes". *State College: Applied Research Laboratory*.

van Dijk, A., & Nieuwstadt, F. (2004). "The calibration of (multi-)hot-wire probes". 2. Velocity-calibration. Utrecht, The Netherlands: *Springer-Verlag*.

von Klemperer, C., & Verijenko, V. (2001). "Design, analysis and construction of a composite camera gimbal". Durban, South Africa: *Elsevier Science Ltd*.

White, F. M. (2011). *Fluid Mechanics*. New York, New York: *McGraw-Hill*.

Appendix A: Flow Channel Schematic

The figure below shows the dimensioned Solidworks drawing of the flow channel. This drawing

was sent to the manufacturer, along with a detailed description of essential design characteristics.
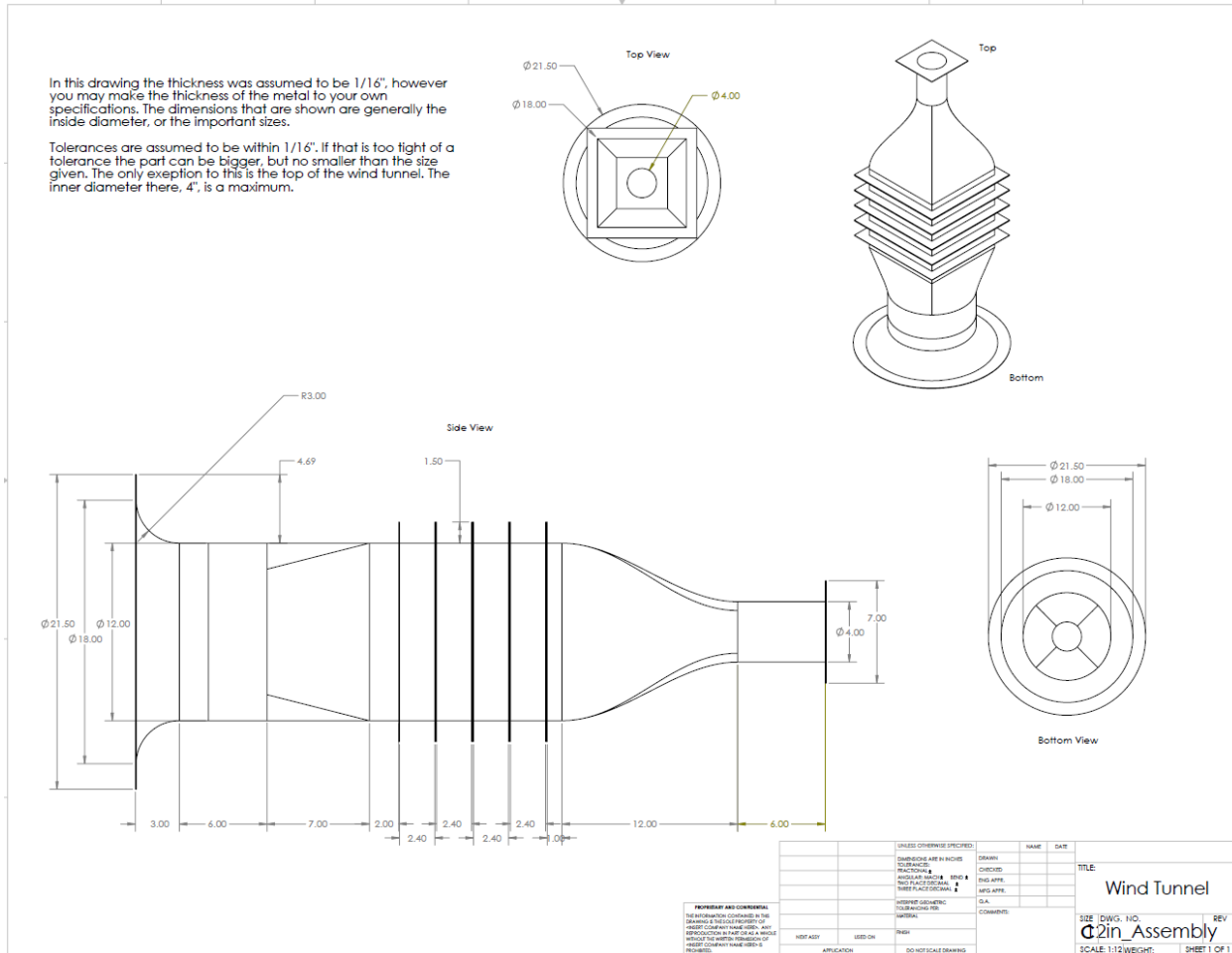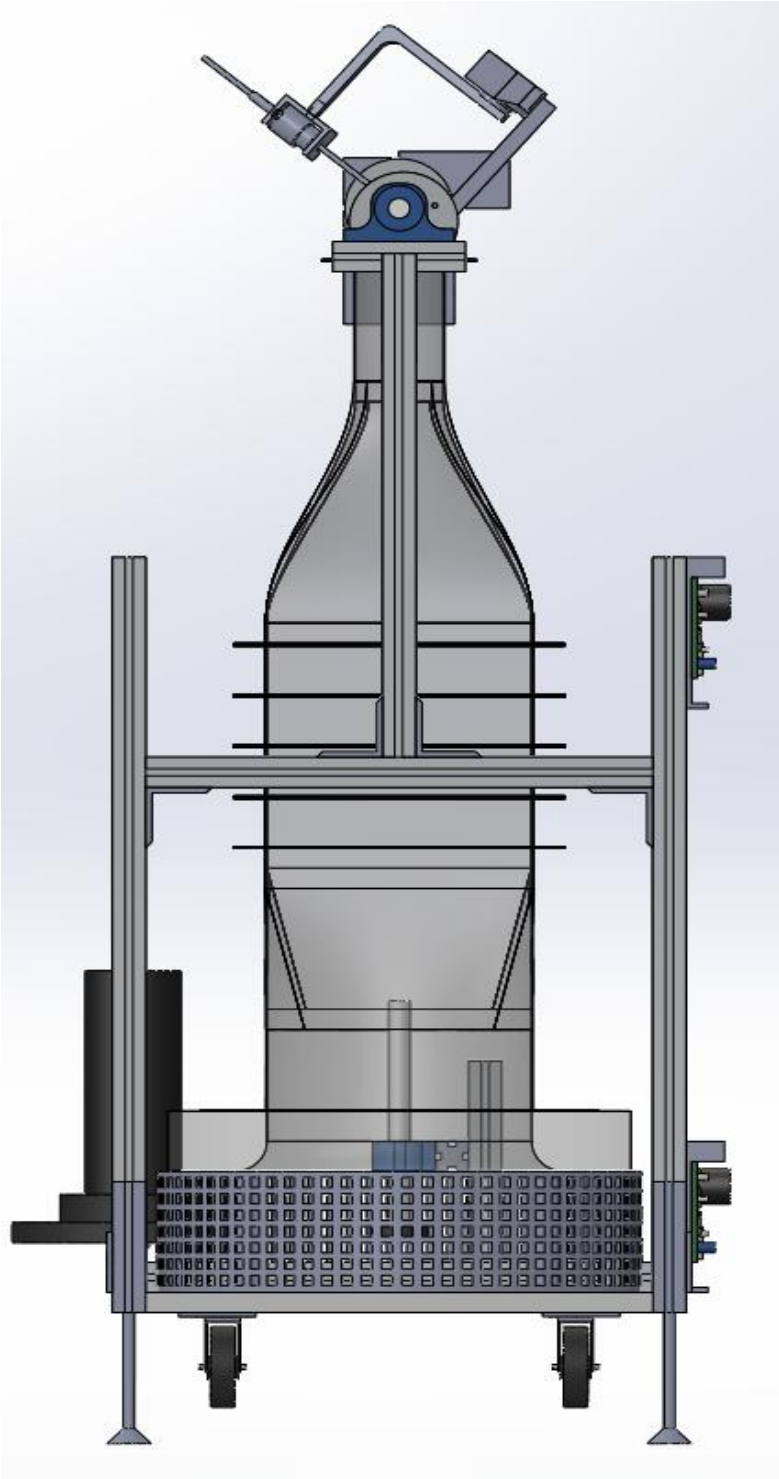
Appendix B: 3-View Model of the Velocity Probe Calibration Rig

The figure below shows the front view of the Solidworks model created of the Velocity Probe Calibration Rig.
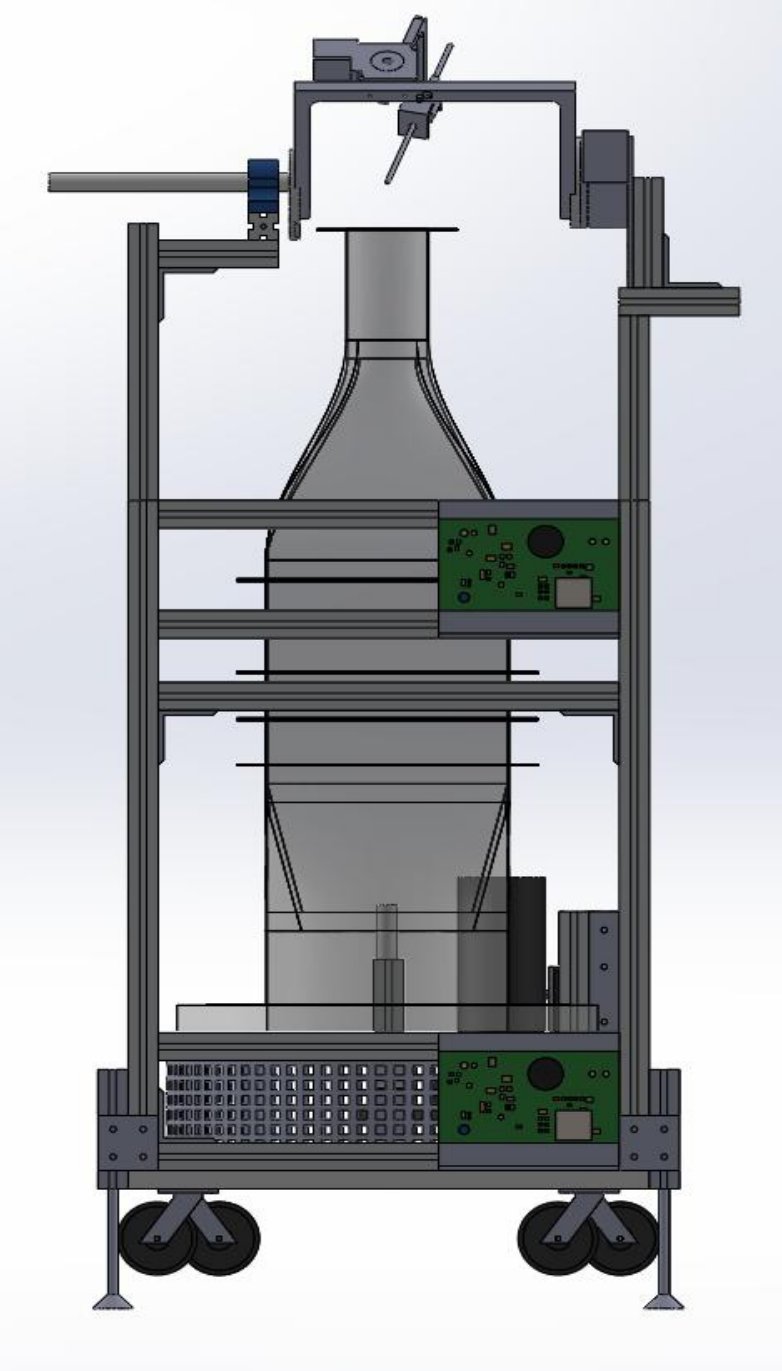
The figure below shows the side view of the Solidworks model created of the Velocity Probe

Calibration Rig.

The figure below shows an isometric view of the Solidworks model created of the Velocity

Probe Calibration Rig.